Systemic Leukocyte-Directed siRNA Delivery Revealing Cyclin D1 as an Anti-Inflammatory Target

Dan Peer, *et al.*

Science **319**, 627 (2008);
DOI: 10.1126/science.1149859

Science (print ISSN 0036-8075; online ISSN 1095-9203) is published weekly, except the last week in December, by the American Association for the Advancement of Science, 1200 New York Avenue NW, Washington, DC 20005.

T_H17 cells. The ability of DCs to induce T_H17 cells was markedly inhibited by cathepsin K inactivation when stimulated with CpG, but not with LPS or PGN (Fig. 3H). Taken together with the results on the role of cathepsin K in CpG-induced cytokine expression in DCs, the impaired induction of T_H17 cells by cathepsin K inactivation was caused, at least in part, by the reduced DC expression of cytokines that are involved in the induction and expansion of T_H17 cells such as IL-6 and IL-23 (*25*, *26*).

Our results show that cathepsin K, which was thought to be an osteoclast-specific enzyme, plays a critical role in the immune system. Cathepsin K functions under the acidified conditions in the endosome, where engagement of CpG by TLR9 occurs, and plays an important role in the signaling events proximal to TLR9. Thus, careful attention should be paid to the side effects of cathepsin K inhibitors on the immune system in the treatment of osteoporosis, whereas they may have dual benefits in the treatment of autoimmune arthritis, the pathogenesis of which is dependent on both DCs and osteoclasts (*9*).

References and Notes

1. J. Banchereau, V. Pascual, A. K. Palucka, *Immunity* **20**, 539 (2004).
2. R. M. Steinman, D. Hawiger, M. C. Nussenzweig, *Annu. Rev. Immunol.* **21**, 685 (2003).
3. V. Turk, B. Turk, D. Turk, *EMBO J.* **20**, 4629 (2001).
4. K. Honey, A. Y. Rudensky, *Nat. Rev. Immunol.* **3**, 472 (2003).
5. P. Saftig *et al.*, *Proc. Natl. Acad. Sci. U.S.A.* **95**, 13453 (1998).
6. B. D. Gelb, G. P. Shi, H. A. Chapman, R. J. Desnick, *Science* **273**, 1236 (1996).
7. W. Chen *et al.*, *Hum. Mol. Genet.* **16**, 410 (2007).
8. M. Asagiri, H. Takayanagi, *Bone* **40**, 251 (2007).
9. H. Takayanagi, *Nat. Rev. Immunol.* **7**, 292 (2007).
10. Y. Yasuda, J. Kaleta, D. Brömme, *Adv. Drug Deliv. Rev.* **57**, 973 (2005).
11. S. Ochi *et al.*, *Proc. Natl. Acad. Sci. U.S.A.* **104**, 11394 (2007).
12. R. Holmdahl *et al.*, *Immunol. Rev.* **184**, 184 (2001).
13. A. Marshak-Rothstein, *Nat. Rev. Immunol.* **6**, 823 (2006).
14. S. Akira, S. Uematsu, O. Takeuchi, *Cell* **124**, 783 (2006).
15. A. Iwasaki, R. Medzhitov, *Nat. Immunol.* **5**, 987 (2004).
16. R. J. Riese *et al.*, *J. Clin. Invest.* **101**, 2351 (1998).
17. S. B. Su *et al.*, *J. Immunol.* **175**, 6303 (2005).
18. A. M. Krieg, *Annu. Rev. Immunol.* **20**, 709 (2002).
19. A. Ronaghy *et al.*, *J. Immunol.* **168**, 51 (2002).
20. E. Latz *et al.*, *Nat. Immunol.* **8**, 772 (2007).
21. I. Mellman, R. M. Steinman, *Cell* **106**, 255 (2001).
22. T. Nakamura *et al.*, *Cell* **130**, 811 (2007).
23. M. Prinz *et al.*, *J. Clin. Invest.* **116**, 456 (2006).
24. B. M. Segal, J. T. Chang, E. M. Shevach, *J. Immunol.* **164**, 5683 (2000).
25. H. Park *et al.*, *Nat. Immunol.* **6**, 1133 (2005).
26. E. Bettelli *et al.*, *Nature* **441**, 235 (2006).

27. We thank K. Takeda, M. Yamamoto, H. Oda, S. Imajoh-Ohmi, M. Matsuura, K. Nishioka, T. Kanda, K. Sato, S. Hida, Y. Iwai, H. Hemmi, H. Yanai, S. Kano, Y. Omatsu, T. Onodera, T. Honda, and A. Suematsu for discussion and assistance. This work was supported in part by a Grant-in-Aid for Creative Scientific Research from the Japan Society for the Promotion of Science (JSPS); grants for the Genome Network Project from the Ministry of Education, Culture, Sports, Science and Technology of Japan (MEXT); Grants-in-Aid for Scientific Research from JSPS and MEXT; Health Sciences Research Grants from the Ministry of Health, Labor and Welfare of Japan; and grants from the Deutsche Forschungsgemeinschaft and the NIH.

Supporting Online Material

www.sciencemag.org/cgi/content/full/319/5863/624/DC1
Materials and Methods
Figs. S1 to S12
References

5 September 2007; accepted 14 December 2007
10.1126/science.1150110

Systemic Leukocyte-Directed siRNA Delivery Revealing Cyclin D1 as an Anti-Inflammatory Target

Dan Peer,[1] Eun Jeong Park,[1] Yoshiyuki Morishita,[1] Christopher V. Carman,[2] Motomu Shimaoka[1]*

Cyclin D1 (CyD1) is a pivotal cell cycle–regulatory molecule and a well-studied therapeutic target for cancer. Although CyD1 is also strongly up-regulated at sites of inflammation, its exact roles in this context remain uncharacterized. To address this question, we developed a strategy for selectively silencing CyD1 in leukocytes in vivo. Targeted stabilized nanoparticles (tsNPs) were loaded with CyD1–small interfering RNA (siRNA). Antibodies to β_7 integrin (β_7 I) were then used to target specific leukocyte subsets involved in gut inflammation. Systemic application of β_7 I-tsNPs silenced CyD1 in leukocytes and reversed experimentally induced colitis in mice by suppressing leukocyte proliferation and T helper cell 1 cytokine expression. This study reveals CyD1 to be a potential anti-inflammatory target, and suggests that the application of similar modes of targeting by siRNA may be feasible in other therapeutic settings.

RNA interference (RNAi) has emerged as a powerful strategy for suppressing gene expression, offering the potential to dramatically accelerate in vivo drug target validation, as well as the promise to create novel therapeutic approaches if it can be effectively applied in vivo (*1*). Cyclin D1 (CyD1) is a key cell cycle–regulating molecule that governs the proliferation of normal and malignant cells (*2*, *3*). In inflammatory bowel diseases, colon-expressed CyD1 is aberrantly up-regulated in both epithelial and immune cells (*4*, *5*). Although CyD1 has also been implicated in promoting epithelial colorectal dysplasia and carcinogenesis, it is not clear whether leukocyte-expressed CyD1 contributes directly to the pathogenesis of inflammation and whether it might serve as a therapeutic target.

To address these questions, we used RNAi silencing of CyD1 in an experimental model of intestinal inflammation. A major limitation to the use of RNAi in vivo is the effective delivery of siRNAs to the target cells (*6*, *7*). RNAi in leukocytes, a prime target for anti-inflammatory therapeutics, has remained particularly challenging, as these cells are difficult to transduce by conventional transfection methods and are often disseminated throughout the body, thus requiring systemic delivery approaches (*8*). One possibility is to use integrins, which are an important family of cell-surface adhesion molecules, as targets for siRNA delivery (*8*). Specifically, we have shown that antibody-protamine fusion proteins directed to the lymphocyte function-associated antigen–1 (LFA-1) integrin selectively delivered siRNAs to leukocytes, both in vitro and in vivo (*8*). However, whether an integrin-directed siRNA delivery approach can induce

[1]Immune Disease Institute and Department of Anesthesia, Harvard Medical School, 200 Longwood Avenue, Boston, MA 02115, USA. [2]Department of Medicine, Beth Israel Deaconess Medical Center, and Harvard Medical School, 330 Brookline Avenue, Boston, MA 02215, USA.

*To whom correspondence should be addressed. E-mail: shimaoka@cbrinstitute.org

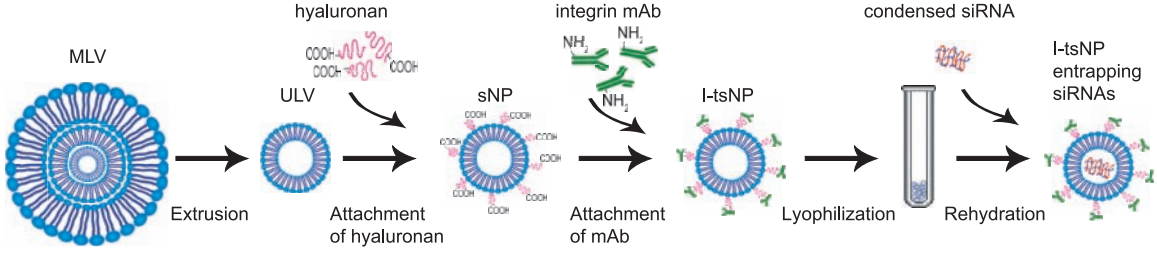

Fig. 1. The processes involved in generating I-tsNPs. Multilamellar vesicle (MLV) [prepared as described in (*9*)] is extruded to form a unilamellar vesicle (ULV) with a diameter of ~100 nm. Hyaluronan is covalently attached to DPPE in the ULV. A monoclonal antibody (mAb) to the integrin is covalently attached to hyaluronan, generating I-tsNP. siRNAs are entrapped by rehydrating lyophilized β_7 I-tsNP with water containing protamine-condensed siRNAs.

sufficiently robust silencing in vivo remains to be seen.

Building on the premise of integrin-targeted siRNA delivery, we developed liposome-based, β_7 integrin–targeted, stabilized nanoparticles (β_7 I-tsNPs) that entrap siRNAs (Fig. 1) (*9*). We began with nanometer-scale (~80 nm) liposomes, formed from neutral phospholipids to circumvent the potential toxicity common to cationic lipids and polymers used for systemic siRNA delivery (*10*). Hyaluronan was then attached to the outer surface of the liposomes, through covalent linkage to dipalmitoylphosphatidylethanolamine (DPPE), thereby stabilizing the particles both during subsequent siRNA entrapment (Fig. 1) and during systemic circulation in vivo (*11*). The resulting stabilized nanoparticles (sNPs) were successfully equipped with a targeting capacity by covalently attaching a monoclonal antibody against the integrins to hyaluronan (fig. S1). The antibody FIB504 (*12*) was selected to direct particles to β_7 integrins, which are highly expressed in gut mononuclear leukocytes (*13*).

We condensed siRNAs with protamine, a positively charged protein that has been used to enhance delivery of nucleic acids [e.g., DNA (*14*) and siRNA (*15*)]. β_7 I-tsNPs were loaded with siRNA cargo by rehydrating lyophilized particles in the presence of condensed siRNAs (*9*), thereby achieving ~80% entrapment efficacy while maintaining the nanodimensions of the particles (tables S1 and S2). β_7 I-tsNPs showed a measurable increase in their capacity to entrap siRNAs such that I-tsNPs carried ~4000 siRNA molecules per particle (~100 siRNA molecules per targeting antibody molecule) (table S1), as compared to an integrin-targeted single-chain antibody protamine fusion protein, which carried five siRNA molecules per fusion protein (*8*). The presence of hyaluronan was critical to maintaining the structural integrity of I-tsNPs during the cycle of lyophilization and rehydration (table S3 and fig. S2).

Cy3-siRNA encapsulated within β_7 I-tsNPs was efficiently bound and delivered to wild-type (WT) but not to β_7 integrin knockout (KO) splenocytes (Fig. 2A). Upon cell binding, β_7 I-tsNPs readily internalized and released Cy3-siRNA to the cytoplasm of both WT splenocytes (Fig. 2B) and the TK-1 lymphocyte cell line (fig. S3) but not that of β_7 integrin KO cells (Fig. 2B). Neither naked siRNA nor isotype control immunoglobulin G (IgG)–attached stabilized nanoparticles (IgG-sNPs) delivered Cy3-siRNA above background levels (Fig. 2, A and B). Using siRNA to Ku70, a ubiquitously expressed nuclear protein and reference target, we showed that Ku70-siRNA delivered by β_7 I-tsNPs induced potent gene silencing in splenocytes, whereas naked or IgG-sNP–formulated Ku70-siRNA did not (Fig. 2C) (additional results in figs. S4 to S7).

To investigate the ability of β_7 I-tsNPs to silence genes in vivo, we administered Ku70-siRNAs (2.5 mg per kilogram of body weight) entrapped in β_7 I-tsNPs by intravenous injection into mice and tested Ku70 expression in mononuclear leukocytes isolated from the gut and spleen after 72 hours (Fig. 2D) (*9*). Ku70-siRNAs delivered by β_7 I-tsNPs potently suppressed Ku70 expression in cells from the gut (including lamina propria and intraepithelial lymphocyte compartments) and spleen. No silencing was observed in cells from identically treated β_7 integrin KO mice, confirming the specificity to the β_7 integrin–expressing cells. Furthermore, naked siRNA as well as siRNA delivered in IgG-sNPs failed to induce detectable silencing in WT or KO mice.

We subsequently examined the biodistribution of ^{3}H-hexadecylcholesterol–labeled nanoparticles intravenously injected into healthy or diseased mice suffering from dextran sodium sulfate (DSS)–induced colitis (Fig. 2E) (*9*). IgG-sNPs showed very little distribution to the gut regardless of the presence of colitis. By contrast, a substantial portion (~10%) of β_7 I-tsNPs spread to the gut in healthy mice. The biodistribution of β_7 I-tsNPs to the gut selectively increased ~3.5-fold in the presence of colitis.

Using β_7 I-tsNPs, we next studied the effects of silencing by CyD1-siRNA (*9*). Treatment with β_7 I-tsNP–entrapped CyD1-siRNA reduced CyD1

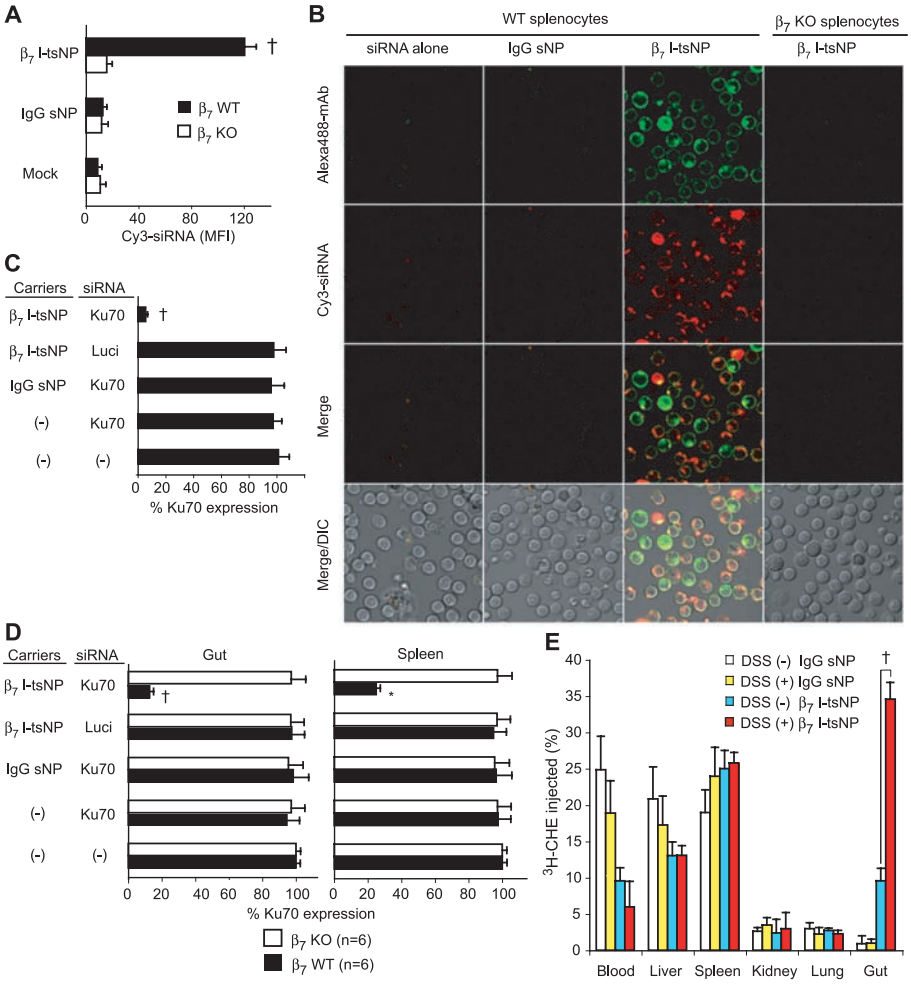

Fig. 2. β_7 I-tsNP delivers siRNAs in leukocytes in a β_7-specific manner. (**A**) Cy3-siRNA delivery via β_7 I-tsNP to WT, but not to β_7 knockout (KO), splenocytes as revealed by flow cytometry. (**B**) Confocal microscopy with differential interference contrast (DIC) morphologies showing the β_7 integrin–specific intracellular delivery of Cy3-siRNA. Images were acquired 4 hours after addition to splenocytes of naked Cy3-siRNA or Cy3-siRNA in Alexa 488–labeled β_7 I-tsNPs or IgG-sNPs. (**C**) Ku70-siRNA delivery with β_7 I-tsNP–induced silencing. Splenocytes were treated for 48 hours with 1000 pmol of Ku70-siRNAs or control luciferase (Luci)-siRNAs, delivered as indicated. (**D**) In vivo silencing of Ku70 in mononuclear cells from the gut and spleen of WT, but not KO, mice. siRNAs (2.5 mg/kg) entrapped as indicated were intravenously injected. Seventy-two hours after injection, Ku70 protein expression was determined by immunofluorescent cytometry after cell permeabilization and expressed as a percentage of Ku70 expression in mock-treated samples [(C) and (D)]. Data are expressed as the mean ± SEM of at least three independent experiments [(A), (C), and (D)]. $^*P < 0.05$, $^\dagger P < 0.01$ versus mock-treated samples. (**E**) Biodistribution of ^{3}H-cholesterylhexadecylether (^{3}H-CHE)–labeled nanoparticles in mice with or without DSS-induced colitis. Pharmacokinetics and biodistribution were determined 12 hours after injection in a total of six mice per group in three independent experiments. Half-lives of β_7 I-tsNP in the blood of healthy and diseased mice were 4.3 and 1.8 hours, respectively. Preferential redistribution of β_7 I-tsNP to the inflamed gut is potentially advantageous for delivering siRNAs to treat intestinal inflammation. $^\dagger P < 0.01$.

mRNA expression in stimulated splenocytes, leading to potent suppression of proliferation (Fig. 3A). β_7 I-tsNPs–entrapped CyD1-siRNA (2.5 mg/kg) was then administered intravenously. Three days later, splenic and gut mononuclear leukocytes from mice treated with β_7 I-tsNP–entrapped CyD1-siRNA showed significantly decreased CyD1 mRNA and reduced proliferation (Fig. 3A).

Although CyD1-knockdown blocked agonist-enhanced expression of the T helper cell 1 (T_H1) cytokines interferon-γ (IFN-γ), interleukin-2 (IL-2), IL-12, and tumor necrosis factor–α (TNF-α), it did not alter the expression of the T_H2 cytokines IL-4 and IL-10 in either CD3/CD28- or phorbol 12-myristate 13-acetate (PMA)/ionomycin-stimulated splenocytes (Fig. 3B and fig. S8) or in PMA/ionomycin-stimulated TK-1 cells (fig. S9). The preferential inhibition of T_H1 cytokines was not observed with the CyD2- or CyD3-knockdown (fig. S9). To investigate whether the CyD1-knockdown suppressed T_H1 cytokine expression independently of its inhibitory effects on the cell cycle, we treated TK-1 cells with aphidicolin to arrest the cell cycle independently of the CyD1 status (Fig. 3C) (*9*). In aphidicolin-treated cells, PMA/ionomycin up-regulated CyD1 as well as T_H1 and T_H2 cytokines. CyD1-knockdown selectively suppressed T_H1 cytokine mRNA expression in aphidicolin-treated and PMA/ionomycin-activated cells (Fig. 3C). This cell cycle–independent suppression of T_H1 cytokines was also seen with the individual applications of four different CyD1-siRNAs that targeted non-overlapping sequences in CyD1 mRNA (Fig. 3D), thereby ruling out the possibility that the blockade of T_H1 cytokines was due to an off-target effect. Thus, CyD1-knockdown could preferentially suppress pro-inflammatory T_H1 cytokine expression independently of any changes in the cell cycle.

We next studied CyD1-knockdown with β_7 I-tsNPs in vivo in DSS-induced colitis (*9*). Mice were intravenously injected with CyD1-siRNA (2.5 mg/kg) entrapped in β_7 I-tsNPs or IgG-sNPs at days 0, 2, 4, and 6. β_7 I-tsNP–delivered CyD1-siRNA potently reduced CyD1 mRNA to a level comparable with that of the uninflamed gut (Fig. 4D). CyD1-knockdown concomitantly suppressed mRNA expression of TNF-α and IL-12, but not of IL-10 (Fig. 4D). Notably, β_7 I-tsNP–delivered CyD1-siRNA led to a drastic reduction in intestinal tissue damage, to a potent suppression of leukocyte infiltration into the colon, and to a reversal in body weight loss and hematocrit reduction (Fig. 4, A to C, and fig. S10). The gut tissue of CyD1-siRNA/β_7 I-tsNP–treated animals exhibited normal numbers of mononuclear cells (Fig. 4C), suggesting that CyD1-knockdown does not induce pathologic cell death in the gut. CyD1-siRNAs entrapped in IgG-sNPs did not induce silencing in the gut, failing to alter cytokine expression in the gut or to reverse manifestations of colitis (Fig. 4, A to C) (additional results in figs. S11 and S12).

The anti-inflammatory effects of CyD1-knockdown in colitis are likely to be mediated both by suppressing the aberrant proliferation of mucosal mononuclear leukocytes and by reducing the expression of TNF-α and IL-12, two pro-inflammatory T_H1 cytokines that are critical to the pathogenesis of colitis. The T_H2 cytokine IL-10 has been shown to suppress inflammation in colitis (*16*). Thus, its transformation from a relatively T_H1-dominant to a more T_H2-dominant phenotype appears to represent a critical and unexpected component of the potent colitis inhibition resulting from CyD1-knockdown. An important future goal will be to elucidate the molecular mechanisms underlying the effects of CyD1-knockdown, both on the induction of T_H2 polarization and on the specific type(s) of leukocytes responsible for reversal of colitis.

Entrapment of condensed siRNA inside these nanoparticles, in tandem with the targeting of the leukocyte β_7 integrin, which readily internalizes bound particles, enabled both highly efficient intracellular delivery and gene silencing in vivo. An effective in vivo siRNA dose of 2.5 mg/kg is one of the lowest doses reported to date for systemically targeted siRNA-delivery applications (*17*–*22*). Compared to other strategies, tsNPs offer the combined benefits of low off-target/toxicity with high cargo capacity (~4000 siRNA molecules per NP). Encapsulation of siRNA within the tsNPs seems to both protect siRNA from degradation (fig. S5) and prevent triggering of unwanted interferon responses (fig. S6). Antibodies coated on the outer surface of the NPs provided selective cellular targeting, while cell surface integrins proved to be effective anti-

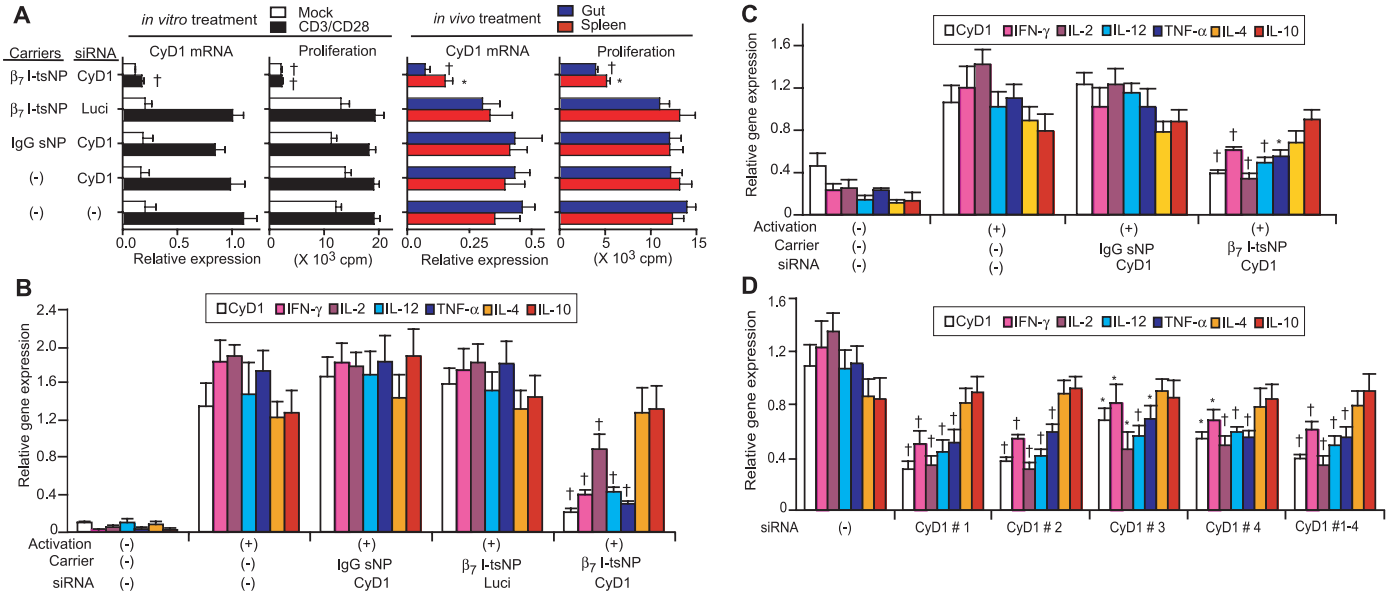

Fig. 3. Silencing of CyD1 by siRNA delivery with β_7 I-tsNPs and its effects on cytokine expression. (**A**) Silencing of CyD1 [measured by quantitative reverse transcription–polymerase chain reaction (qRT-PCR)] and its effects on proliferation (measured by [^{3}H]-thymidine incorporation). In in vitro treatments, splenocytes were examined after 72 hours' incubation with 1000 pmol of siRNAs delivered as indicated in the presence or absence of CD3/CD28 stimulation. In in vivo treatments, siRNAs (2.5 mg/kg) entrapped as indicated were intravenously injected into a total of six mice per group in three independent experiments. Seventy-two hours later, mononuclear cells harvested from the gut and spleen were examined. $^*P < 0.05$, $^\dagger P < 0.01$ versus mock-treated samples. (**B**) CyD1-knockdown selectively suppresses T_H1 cytokine mRNA expression in splenocytes activated via CD3/CD28. (**C**) CyD1-knockdown selectively suppresses T_H1 cytokine mRNA expression independently of its inhibitory effects on the cell cycle. In aphidicolin-treated TK-1 cells, in which the cell cycle was arrested, PMA/ionomycin–up-regulated T_H1 cytokine mRNA expression was selectively suppressed by CyD1-knockdown. (**D**) Cell cycle–independent suppression of T_H1 cytokines observed with individual applications of four different CyD1-siRNAs. (C) to (D) TK-1 cells were first treated for 12 hours with aphidicolin then with siRNAs (1000 pmol) delivered as indicated for another 12 hours in the presence of PMA/ionomycin and aphidicolin. (B) to (D) $^*P < 0.05$, $^\dagger P < 0.01$ versus mock-treated activated cells. (A) to (D) mRNA levels for CyD1 and cytokines were measured by qRT-PCR. Data are expressed as the mean ± SEM of at least three independent experiments.

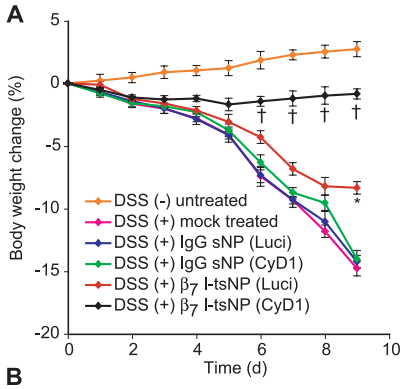

B

Mice treatment	HCT (mean ± SEM) (%)
DSS (-) untreated	57.2 ± 0.9
DSS (+) mock treated	40.4 ± 3.4
DSS (+) IgG sNP (Luci)	39.9 ± 3.9
DSS (+) IgG sNP (CyD1)	43.5 ± 2.6
DSS (+) β_7 I-tsNP (Luci)	45.7 ± 7.3
DSS (+) β_7 I-tsNP (CyD1)	53.2 ± 1.7 †

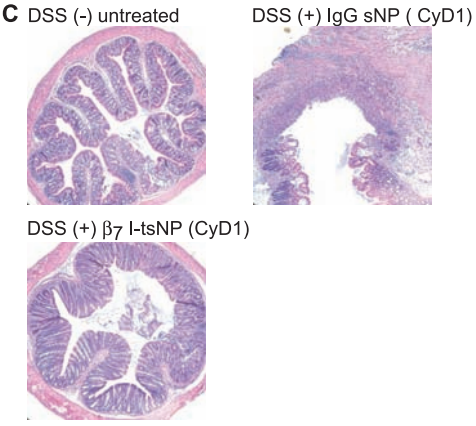

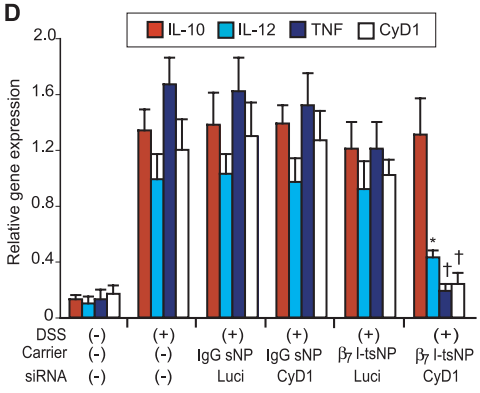

Fig. 4. Cyclin-D1–siRNA delivered by β_7 I-tsNP alleviated intestinal inflammation in DSS-induced colitis. Mice were intravenously administered CyD1- or luciferase (Luci)-siRNAs (2.5 mg/kg) entrapped in either β_7 I-tsNPs or IgG-sNPs, or naked CyD1-siRNA (2.5 mg/kg) at days 0, 2, 4, and 6 (a total of six mice per group in three independent experiments). (**A**) Change in body weight. (**B**) Hematocrit (HCT) measured at day 9. (**C**) Representative histology at day 9 (hematoxylin and eosin staining, magnification ×100). (**D**) mRNA expression of CyD1 and cytokines in the gut. mRNA expression was measured by qRT-PCR with homogenized colon samples harvested at day 9. (A), (B), and (D) Data are expressed as the mean ± SEM of three independent experiments. *$P < 0.05$, †$P < 0.01$ versus mock-treated mice with DSS-induced colitis.

body targets for both delivery and uptake of tsNPs. Thus, the I-tsNP approach may have broad applications not only for in vivo drug target validation, but also for potential therapies that are not limited to leukocytes or inflammatory settings.

References and Notes

1. E. Iorns, C. J. Lord, N. Turner, A. Ashworth, *Nat. Rev. Drug Discov.* **6**, 556 (2007).
2. D. W. Stacey, *Curr. Opin. Cell Biol.* **15**, 158 (2003).
3. M. Fu, C. Wang, Z. Li, T. Sakamaki, R. G. Pestell, *Endocrinology* **145**, 5439 (2004).
4. R. Yang, W. Bie, A. Haegebarth, A. L. Tyner, *Cell Cycle* **5**, 180 (2006).
5. H. van Dekken *et al.*, *Acta Histochem.* **109**, 266 (2007).
6. M. A. Behlke, *Mol. Ther.* **13**, 644 (2006).
7. D. M. Dykxhoorn, J. Lieberman, *Annu. Rev. Biomed. Eng.* **8**, 377 (2006).
8. D. Peer, P. Zhu, C. V. Carman, J. Lieberman, M. Shimaoka, *Proc. Natl. Acad. Sci. U.S.A.* **104**, 4095 (2007).
9. Materials and methods are available as supporting material on *Science* Online.
10. C. R. Dass, *J. Mol. Med.* **82**, 579 (2004).
11. D. Peer, A. Florentin, R. Margalit, *Biochim. Biophys. Acta* **1612**, 76 (2003).
12. D. P. Andrew *et al.*, *J. Immunol.* **153**, 3847 (1994).
13. S. K. Shaw, M. B. Brenner, *Semin. Immunol.* **7**, 335 (1995).
14. F. L. Sorgi, S. Bhattacharya, L. Huang, *Gene Ther.* **4**, 961 (1997).
15. S. D. Li, L. Huang, *Mol. Pharm.* **3**, 579 (2006).
16. J. O. Lindsay, A. Sandison, P. Cohen, F. M. Brennan, H. J. Hodgson, *Dig. Dis. Sci.* **49**, 1327 (2004).
17. J. Soutschek *et al.*, *Nature* **432**, 173 (2004).
18. D. V. Morrissey *et al.*, *Nat. Biotechnol.* **23**, 1002 (2005).
19. R. M. Schiffelers *et al.*, *Nucleic Acids Res.* **32**, e149 (2004).
20. E. Song *et al.*, *Nat. Biotechnol.* **23**, 709 (2005).
21. F. Takeshita *et al.*, *Proc. Natl. Acad. Sci. U.S.A.* **102**, 12177 (2005).
22. J. D. Heidel *et al.*, *Proc. Natl. Acad. Sci. U.S.A.* **104**, 5715 (2007).

23. We thank J. Lieberman for critically reading manuscript and discussion; R. Margalit, R. S. Langer, and P. Sicinski for discussions; and Y. Imai, A. Zur, P. Sage, and R. Yoo for technical assistance. D.P. is supported by the Dorot Foundation and Pfizer Inc. Y.M. is supported by the Uehara Memorial Foundation. This work was supported by the Arthritis Foundation (C.V.C.) and NIH grants HL048675 and AI63421 (M.S.).

Supporting Online Material

www.sciencemag.org/cgi/content/full/319/5863/627/DC1
Materials and Methods
Figs. S1 to S12
Tables S1 to S3
References

29 August 2007; accepted 18 December 2007
10.1126/science.1149859

Direct Observation of Hierarchical Folding in Single Riboswitch Aptamers

William J. Greenleaf,[1*] Kirsten L. Frieda,[2] Daniel A. N. Foster,[4] Michael T. Woodside,[4,5*†] Steven M. Block[1,3†]

Riboswitches regulate genes through structural changes in ligand-binding RNA aptamers. With the use of an optical-trapping assay based on in situ transcription by a molecule of RNA polymerase, single nascent RNAs containing *pbuE* adenine riboswitch aptamers were unfolded and refolded. Multiple folding states were characterized by means of both force-extension curves and folding trajectories under constant force by measuring the molecular contour length, kinetics, and energetics with and without adenine. Distinct folding steps correlated with the formation of key secondary or tertiary structures and with ligand binding. Adenine-induced stabilization of the weakest helix in the aptamer, the mechanical switch underlying regulatory action, was observed directly. These results provide an integrated view of hierarchical folding in an aptamer, demonstrating how complex folding can be resolved into constituent parts, and supply further insights into tertiary structure formation.

Riboswitches are elements of mRNA that regulate gene expression through ligand-induced changes in mRNA secondary or tertiary structure (*1*, *2*). This regulation is accomplished through the binding of a small metabolite to an aptamer in the 5′-untranslated region of the mRNA, which causes conformational changes that alter the expression of downstream genes. Riboswitch-dependent regulatory processes depend crucially on the properties of aptamer folding; the kinetics and thermodynamics of folding are therefore of central importance for understanding function.

Among the simplest riboswitches are those regulating purine metabolism, which have aptamers with "tuning fork" structures (*3*, *4*) that bind ligands at a specific residue in a pocket formed by a three-helix junction. The junction is thought to be preorganized by numerous tertiary contacts, including interactions between two hairpin loops, but the binding pocket itself is likely stabilized only upon ligand binding (*4*–*10*). Ligand binding also stabilizes a nearby helix (*3*–*5*), sequestering residues that would otherwise participate in an alternate structure affecting gene expression (e.g., terminator or anti-terminator hairpins, ribosome binding sequences). Features such as ligand specificity (*6*, *11*) and its structural basis (*6*, *7*), the rates and energies for ligand binding and dissociation (*12*), the kinetics of loop-loop formation (*10*), and the interplay of structural preorganization and induced fit (*7*–*9*) have recently been investigated. These studies, how-